INDIAN JOURNAL OF SCIENCE AND TECHNOLOGY

RESEARCH ARTICLE

Rate Equations Model to Simulate the Performance of Passive Q-Switched Laser with Raman Medium Optical System

Dunya Saad[1], Hussein [1], Abdulkareem Mahdi Salih[1]*

1 Physics Dep. , College of Science , Thi-Qar University, ThiQar, Iraq

OPEN ACCESS

Received: 02-08-2023

Accepted: 14-09-2023

Published: 25-10-2023

Citation: Saad D, H, Salih AM (2023) Rate Equations Model to Simulate the Performance of Passive Q-Switched Laser with Raman Medium Optical System. Indian Journal of Science and Technology 16(39): 3353-3360. https://doi.org/10.17485/IJST/v16i39.1744

* **Corresponding author**.

abdulkareem@sciutq.edu.iq

Funding: None

Competing Interests: None

Published By Indian Society for Education and Environment (iSee)

ISSN
Print: 0974-6846
Electronic: 0974-5645

Abstract

Objective: Mathematical model of rate equations was proposed to simulate the performance of laser system to generate passive Q-switching laser pulse, which interacting with Raman medium to produce Stokes and anti-Stokes pulses. **Methods:** The proposed rate equations model has been tested theoretically in optical system consist of Nd:YVO_4, $PbWO_4$, and Cr^{+4}:YAG as active medium, Raman medium, saturable absorber material respectively. Rung-Kutta–Fehelberg numerical method used in the solve of the model. The results were showed good compatibility compared with those of previous studies. After performance the verification steps, this model was tested in the study of the effect of saturable absorber ions concentration on the characteristics of passive Q-switching, Stokes, anti-Stokes pulses. **Findings:** The proposed rate equations model it is possible adopt in theoretical studies related to high power pulses interaction with Raman medium to generate Stokes and anti-Stokes pulses. **Novelty:** Add new mathematical equations and terms to that of previous mathematical models. The models consist of six equations instead of four or five equations.

Keywords: Laser; Passive QSwitching Pulse; Stokes and Anti-Strokes Pulse

1 Introduction

The high power pulses have many important applications such as industrial, medical, military, space and astronomy, communications and scientific researches[1,2]. For this reason, these pulses have attracted the attention of researchers in practical and theoretical aspects. One the technique in the generation of high power pulses is the passive Q- switching (PQS) technique[3], it involves the additions of saturable absorber material (SA) in the laser system[4]. Integrated performance between SA and the active medium (AM) in the PQS system that produces high power pulses named PQS pulse. In a later development, it was included the PQS system by Raman medium (RM). An interaction will occur between PQS laser pulse and RM. This reaction will produce other pulses in different frequencies , there are called Rayleigh pulse it is represents elastic scattering characterized by the same frequency of PQS wave, Stokes pulse which

is represent inelastic scattering and characterized by less frequency of incident wave (PQS laser wave) and anti- Stokes pulses which is also represent inelastic scattering and characterized by more of frequency comparing with incident wave as shown in Figure 1 [5].

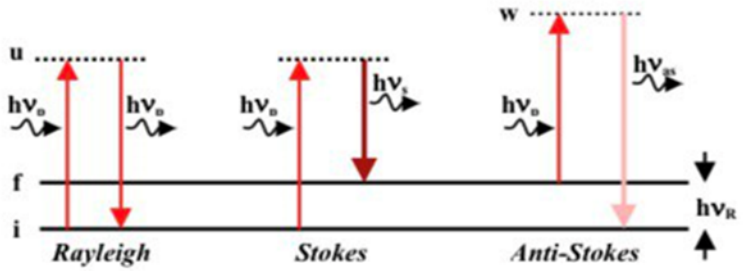

Fig 1. Rayleigh, Stokes, and anti-Stokes scattering

The mathematical expression of PQS wave-RM was represented in equation 1 [6].

$$\vec{P} = \alpha_0 \vec{E}_P \cos(2\pi v_p t) + \left[\frac{\partial \alpha}{\partial Q}\left(\frac{\vec{E}_P Q_0}{2}\right)(\cos(2\pi(v_p - v_{vi\,b})t) + \cos(2\pi(v_p + v_{vi\,b})t)\right] \quad (1)$$

Where $\vec{P}$ represents the nonlinear polarization in medium, the first, second and the third terms represents Rayleigh, Stokes and anti- Stokes scattering respectively [6].

In this study used neodymium doped yttrium orthovanadate (Nd:YVO_4) as AM of system. Figure 2 shows the energy levels diagram of Nd:YVO_4 [7] the transition from energy levels lead to laser. The chromium doped Yttrium Aluminum Garnet (Cr^{+4}:YAG) used as the SA. Figure 3 shows the energy levels diagram of Cr^{+4}:YAG the energy levels E_1, E_2 are responsible for absorbing laser photons. While lead tungstate ($PbWO_4$) crystal used as the RM.

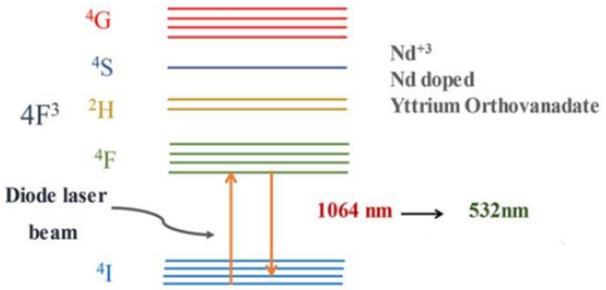

Fig 2. Nd:YVO_4 energy level diagram [7]

2 Methodology

Rate equations model was proposed in this study to simulate the interconnected performance of the three elements (AM, SA, and RM) with other components of optical system in order to generates PQS, Stokes, and anti-Stokes pulses. The novelty of model included six rate equations, it is represents the development of rate equations models consisting of five equations as the reference [10], or four equations as the reference [11]. In order to as certain the physical concepts and the mathematical relations

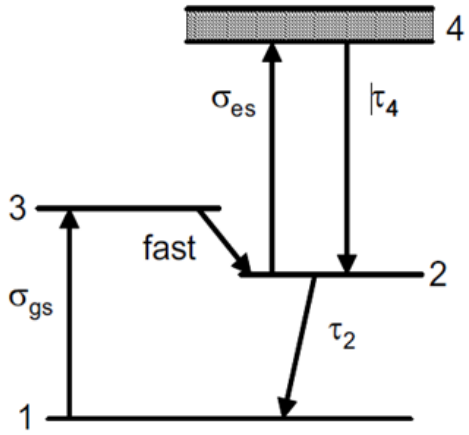

Fig 3. Cr^{+4}: YAG energy level diagram [8,9]

of this model, the model was tested theoretically by numerical simulation of a laser system consist of Nd:YVO_4 used as AM and Cr^{+4}: YAG as a SA, and $PbWO_4$ crystal used as the RM. showed good agreement with studies which dealt the Stokes anti-Stokes pulses generation by Raman scattering theory as shown in reference exhibit a steeper gaussian pulse shape and smoother pulse edges.as shown in ref[12]. Also the results of simulation showed good agreement with physical concepts in second and third terms of Eq.1. pulse, while the energy of the anti-Stock pulse increases than the energy of the PQS pulse, the value of the energy of PQS pulse, the Stokes pulse, and the anti-Stock pulse is 1.328 and 1.12 and 1.554 mJ.

Theory

The proposed rate equations model as the following:

$$\frac{d\emptyset_L}{dt} = \emptyset_L \left[k_g N_g - k_a N_{ag} - \beta k_a N_{ae} - \frac{2ghcv_s \emptyset_s l_R}{\tau_{Rt}} - \frac{2ghcv_{as} \emptyset_{as} l_R}{\tau_{Rt}} - \frac{1}{\tau_L} \right] \tag{2}$$

$$\frac{d\varnothing_S}{dt} = \varnothing_S \left(\frac{2ghcv_s \varnothing_L l_R}{\tau_{Rt}} - \ k_a N_{ag} - \beta k_a N_{ae} - \frac{1}{\tau_S} \right] + K_{SP} \varnothing_L \tag{3}$$

$$\frac{d\varnothing_{as}}{dt} = \varnothing_{as} \left(\frac{2ghcv_{as} \varnothing_L l_R}{\tau_{Rt}} - \ k_a N_{ag} - \beta k_a N_{ae} - \frac{1}{\tau_{as}} \right] + K_{SP} \varnothing_L \tag{4}$$

$$\frac{dN_g}{dt} = R_p - \gamma_g N_g - \gamma_p k_g N_g \varnothing_L \tag{5}$$

$$\frac{dN_{ag}}{dt} = -K_a N_{ag} \varnothing_L - k_a N_{ag} \varnothing_s - k_a N_{ag} \varnothing_{as} + \gamma_a N_{ae} \tag{6}$$

$$\frac{dN_{ae}}{dt} = K_a N_{ag} \varnothing_L + K_a N_{ag} \varnothing_s + k_a N_{ag} \varnothing_{as} - \gamma_a N_{ae} - \beta K_a N_{ae} \left(\varnothing_s + \varnothing_{as} \right) \tag{7}$$

Eqs. 2, 3 and 4 describes the time variation of laser photons density, Raman-Stokes photons density and Raman anti-Stokes photons density respectively, Eq. 5 describes the population inversion density and Eq.6,7 describes the time variation of population of SA ground and excite level on receptivity. $\varnothing_L$ (cm^{-3})laser photons density, coupling coefficient $K_g = \frac{2l_g \sigma_g}{\tau_{Rt}} (s^{-1})$, $L_g(cm)$ is length of active medium, $\sigma_g(cm^2)$ is the emission cross section of active medium , N_g (cm^{-3}) is the population inversion density, $K_a = \frac{2l_a \sigma_{ag}}{\tau_{Rt}}$ (s^{-1}) ,$\tau_{Rt} = \frac{2l_c}{c}$ (s) is the life time of photon in cavity, l_c (cm) is cavity length,

σ_{ag} (cm^2) the absorption cross section of ground level of SA, l_a is length of SA ,N_{ag} is population of ground level in SA (cm^{-3}) $\beta = \frac{\sigma_{ae}}{\sigma_{ag}}$, $\sigma_{ae}(cm^2)$ is the absorption cross of excited level of SA, N_{ae} (cm^{-3}) $N_{ag} + N_{ae} = n_i$, where n_i is the total ions density (concentration) of SA, g is (cm/GW) is the Raman gain, h plank constant, c(cm/s) speed of light, v_s (cm^{-1}) the frequency of stokes photon , $v_S = v_L - v_R, v_L$ laser frequency

v_L v_R Raman shift , l_R is Raman medium length, v_{as} $v_{as} = v_l + v_R$, $\tau_L$is the lifetime of laser photon in the cavity $\tau_L = \frac{2L_C}{c[L-ln\sqrt{RR_L}]} \rightarrow \frac{\tau_{RT}}{[L-ln(\sqrt{RR_L})]}$, L(cm) is the round trip losses in the cavity, $\varnothing_S$ *is* Raman-Stokes photons density, k_{sp} is the spontaneous Raman scattering factor (sR_p (s^{-1}) $\gamma_g = \frac{1}{\tau_g}$ (s^{-1}) *is the decay rate of the upper laser level* (*excited level*)τ_g (s) is the life time of excited level, $\gamma_p \gamma_p = 2$ for 3 level system, $\gamma_p = 1$ for 4 level system, R is the reflectivity of total reflection mirror, $R_L \tau_s = \frac{2L_C}{c[L-ln\sqrt{RR_s}]}$ is the round trip losses of Stokes photons of the cavity, R_s $\tau_{as} = \frac{2L_C}{c[L-ln\sqrt{RR_{as}}]}$

is the round trip losses of anti-Stokes in the cavity R_{as} is output coupler reflectivity at anti-Stokes.

It is worth noting, it is imperative to make some physical and mathematical approximation. The first and the second term in Eq.5 can be neglected due the release and emission of PQS pulse in very short time compared to the time influence of the factors R_p, γ_g,[13,14] also the fourth term in the Eq. 6, and the fourth and the fifth terms in Eq.7 can be neglected due to long time decay of excited level of SA (level 2 in Figure 3), and due to very short lifetime of level 4 in Figure 3[15]. At initial time of construction of PQS pulse, Eq. 2 can be equal to zero $\left(\frac{d\phi_L}{dt} \approx 0.\right), N_{ae} \approx 0., N_g = N_{go}, N_{ag} \approx n_i$ then it is possible to appreciate the initial population inversion density N_{go} as the following expression:

$$N_{g0} = \frac{k_a N_{ao} + \left(\frac{(2ghc\, l_R\,(v_s \varnothing_s + v_{as} \varnothing_{as})}{\tau_{RT}}\right) + \frac{1}{\tau_L}}{K_g} \tag{8}$$

As well as at the time becomes that PQS pulse at its peak, Eq. 2 can be equal to zero $\left(\frac{d\phi_L}{dt} \approx 0.\right), N_{ag} \approx 0., N_g = N_{th}, N_{a\varepsilon} \approx n_i$, then it is possible to estimate the threshold population inversion density as the following expression:

$$N_{th} = \frac{\beta K_a N_{a0} + \left(\frac{(2ghc\, l_R\,(v_s \varnothing_s + v_{as} \varnothing_{as})}{\tau_{RT}}\right) + \frac{1}{\tau_L}}{k_g} \tag{9}$$

And after the pulse released, can be estimate the pulse energy (E) as the following expression[16] :

$$E = \frac{(N_{go} - N_{gf})}{N_{go}} \frac{(N_{go} - N_{gf})\, hv}{\gamma} \tag{10}$$

Where N_{gf} it represents the final population inversion density, their value can be determined of the results of the numerical solution of Eq.5 . h Blank constant, v is the frequency. The duration of pulse (τ) as well as can be estimated after the pulse released (from numerical solution results of Eq. 2,3,4), it is represents the pulse width at half maximum (FWHM). The power calculates by the relation:

$$P = \frac{E}{\tau} \tag{11}$$

3 Results and Discussion

Software program has been prepared in this study, after performance the verification steps mentioned in the methodology paragraph, the mathematical model has been solved numerically by Rung-Kutta-Fehelberg method to study the effect of ions density of SA on characteristics of PQS, Stokes, and Anti-Stokes pulses generated from the optical system consist of Nd:YVO_4 used as AM and Cr^{+4}: YAG as aSA, and $PbWO_4$ crystal used as the RM. The input data in Table 1 have been used in the study.

Figures 4 and 5 represent the temporal behavior of the three pulse in terms of two different ions density values of SA. Note from the behavior that the maximum value of the photon density of the generated pulses decreases with the increase in the ions density of SA, it has also been observed that the generation time of the three pulses comes later when the ions density of SA increases as shown in Table 2 and Figure 6.

The study explains that the behavior or characteristics of the Stokes and the anti-Stokes pulse depends on the characteristics of the primary pulse (PQS laser pulse) that interacts with the Raman medium.

Table 1. Input data of computations

Param.	Value	Ref.	Param.	Value	Ref.
K_{sp}	$2 \times 10^{-10} s^{-1}$	(17)	σ_e	$6.5 \times 10^{-19} cm^2$	(18)
v_R	$925\ cm^{-1}$	(17)	σ_{ae}	$0.55 \times 10^{-18} cm^2$	(19)
G	8.4cm/GW	(17)	σ_{ag}	$2.5 \times 10^{-18} cm^2$	(19)

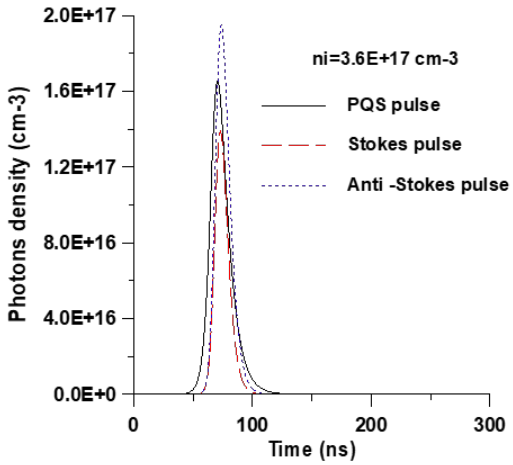

Fig 4. The time variation of pulses photons density

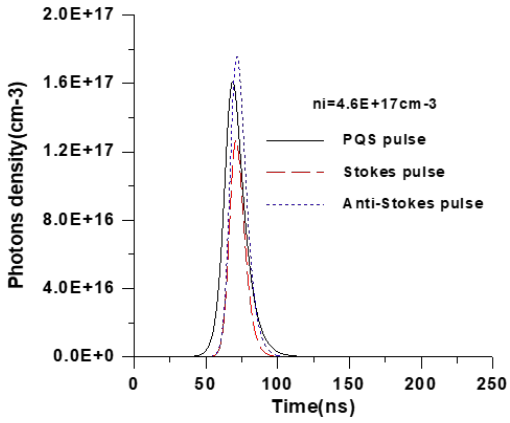

Fig 5. The time variation of pulses photon density

Table 2. Maximum photons density for pulses with the time

Maximum photons values of pulses at			Maximum photons values of pulses at			
Anti-Stokes	Stokes	PSQ	Anti-Stokes	Stokes	PSQ	Pulse type
						Photons density(Cm-3)
72	71	69	74	73	71	Time(ns)

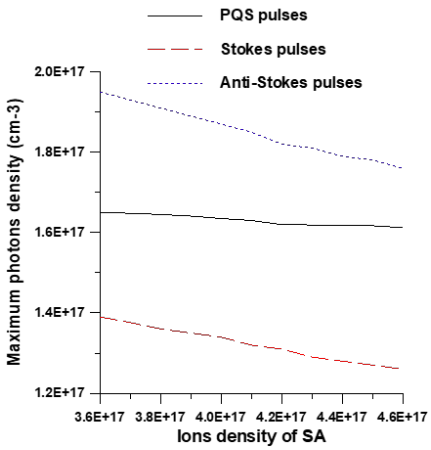

Fig 6. Max. photons density of PQS, Stokes, and anti-Stokes as a function of SA ions density

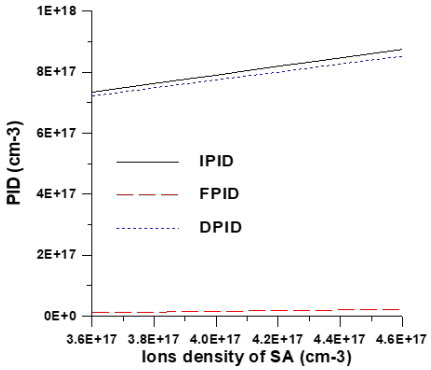

Fig 7. Population inversion density as function of SA ions density

Figure 6 represents the decrease in the maximum values of photons density of the generated pulses in terms of the increase in the density of the absorbent material. The study explains this to the absorption of the laser photons (basic pulse) which oscillating inside the resonator, especially by some ions in the Raman medium which move to spectral lines unrelated to the production of pulses. Figure 7 represents the increment in intensity of the initial population inversion density (IPID) and final population inversion density (FPID) and the difference between them(DPID). The study explains this to the increase in the initial value of the population inversion of the ions of the active medium, which led to a rapid construction of the basic pulse, which in turn led to a rapid construction of the Stokes and anti-Stokes pulse. The idea in following up the difference between the value of the initial and final population inversion is to estimate the amount of energy released from the active medium as a basic pulse that interacts with the ions of the Raman medium.

Figure 8 shows the decreasing in the pulses duration as a function of ions density of SA. The study related that to rapid construction of the basic pulse, which in turn led to a rapid construction of the Stokes and anti-Stokes pulse. The rapid construction of the basic pulse occur due to the increasing in the IPID as shown in Figure 7. Figure 9 shows the increasing in the pulses energy in terms of the increase in the ions density of SA. The study related that due to the increasing in the DPID as shown in Figure 7.

Figure 10 represents the increase in the power of the three pulses in terms of the increase in the ions density of SA. The study explains this because of the increase in the energy of the pulses and the decrease in the duration of the pulses, as shown in Figures 8 and 9, respectively.

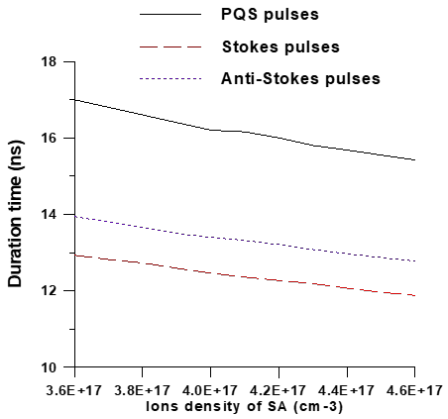

Fig 8. Duration of pulses as a function of ions density of SA

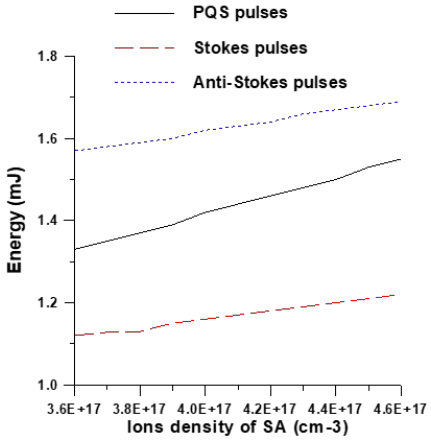

Fig 9. Energy of pulses as function of ions density of SA

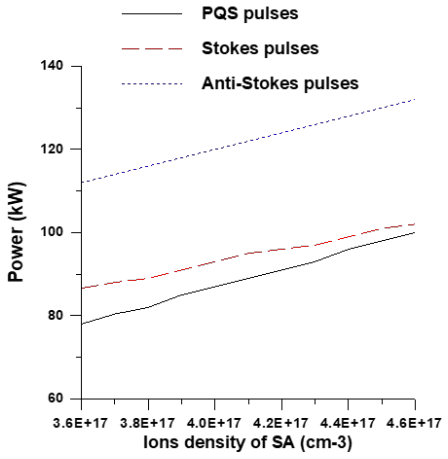

Fig 10. Power of pulses as function of ions density of SA

4 Conclusion

1. The mathematical model of rate equation proposed in this study, it can be employed in the study of the interaction of laser waves with Raman media to simulate the generation of Stokes and anti-Stokes high power pulses in passively Q-switching system.
2. To increase the power of the generated pulses, requires increases in ions density of saturable absorber material which is used in system.

References

1) Jingxuan X, Xu D, Hanming Y. Generation of High Peak Power Pulses With Controllable Repetition Rate in Doubly Q-Switched Laser With AOM/SnSe2. 2022. Available from: https://doi.org/10.3389/fphy.2022.873058.
2) Mikołaj N, Kazimierz J, Daniel K, Marek P, Józef C, J P. Compact and integrated high-power pulse generation and forming system . 2021. Available from: https://doi.org/10.3390/en15010099.
3) Liwei X, Yingyi L, Jun C, Wanli Z, Tongyu L, Tongyu D, et al. Graphen Passively Q-Switched Nd: YAG Laser by 885 nm Laser Diode Resonant Pumping. . Available from: https://doi.org/10.3390/app12168365.
4) Jingcheng S, Tianli F, Shengzhi Z, Tao L, Zhongben P, Andjia Z. Saturable absorption characteristics of Bi 2 Se 3 in a 2 μm Q-switching bulk laser. *Optics Express*. 2020;p. 5639–5647.
5) Young C, Sung S. Fabricating a Raman spectrometer using an optical pickup unit and pulsed power. *Scientific reports*;2020:11692–11692.
6) C, S S. Fabricating a Raman spectrometer using an optical pickup unit and pulsed power. *Scientific reports*;2020:11692–11692.
7) Ahmed S, Osama T, Mohamed S, Ashraf M, Sherbini E, Sherbini TM. Spectral characteristics of a microchip Nd:YVO4 laser. *Journal of Optics*;2022.
8) Giese A, Körber M, Kostourou K, Kopf D, Kottcke M, Lohbreier J, et al. Passively Q-switched sub-100 ps Yb3+: YAG/Cr4+: YAG microchip laser: experimental results and numerical analysis. 2023. Available from: https://doi.org/10.1117/12.2649057.
9) Hiroki T, Christian K, Kannari F. Transition-Metal-Doped Saturable Absorbers For Passive Q-Switching Of Visible Lasers. *Optical Materials Express*. 2020;10(8). Available from: https://doi.org/10.1364/OME.395893.
10) Sally BK, Ms AK. Simulation of Raman spontaneous scattering factor effect on Stoke Raman and passive Q-switching pulses characteristic. *IOP Conference Series: Materials Science and Engineering*. 2020;p. 72160. Available from: https://doi.org/10.1088/1757-899X/928/7/072160.
11) Xiao LW, Jun XJ, D. Sub-nanosecond, high peak power Yb:YAG/Cr4+:YAG/YVO4 passively Q-switched Raman micro-laser operating at 1134 nm. *Journal of Luminescence*. 2021;117955. Available from: https://doi.org/10.1016/j.jlumin.2021.117955.
12) Chengzi H, Qilai Z, Changsheng Y, Wel L, Yuxing S, Jiamin H, et al. Pulse compression of a single-frequency Q-switched fiber laser based on the cascaded four-wave mixing effect. *Optics Express*. 2022;30(20):37101. Available from: https://doi.org/10.1364/OE.470517.
13) Hussein ZA, Salih AK. Investigation of Initial Transmission Effect on Saturable Absorber Optical Performance of Passive Q-Switching Doped Fiber Laser. *NeuroQuantology*. 2021;p. 103–110. Available from: https://doi.org/10.14704/nq.2021.19.7.NQ21090.
14) Hussein TM, Salih AKM. Simulation of Effective Beam Area Ratio Effect on Characteristics of Passive Q-Switched Fiber Doped Laser. *Journal of Optoelectronics Laser*. 2022;41:14. Available from: https://www.gdzjg.org/index.php/JOL/article/view/1286.
15) Alonso VP, Weigand R, Snchez-Balmaseda M, Pérez JMG. Powerful algebraic model to design Q-switched lasers using saturable absorbers. 2023. Available from: https://doi.org/10.1016/j.optlastec.2023.109506.
16) Zainab AH, Ms AK. Saturable absorber initial transmission effect on characteristics of passive Q-switching Er+3doped fiber laser. *AIP Conference Proceedings2022, 2386*. 2022. Available from: https://doi.org/10.1063/5.0067126.
17) Ch YW, In, Takashing O, Mitsuhiro T, Nobou T, Yoshiyuki U. 2001.
18) Chen M, Dai S, Yin H, Zhu S, Li Z, Chen Z. Passively Q-switched yellow laser at 589 nm by intracavity frequency-doubled c-cut composite Nd:YVO4 self-Raman laser. *Optics & Laser Technology*. 2021;133:106534. Available from: https://doi.org/10.1016/j.optlastec.2020.106534.
19) Ruijun L, Fang Z, Zhengping W, Wei X, Hui Y, Tianli F. Efficient near-infrared, multiwavelengths PbWO4 Raman laser. *Optical Engineering*. 2017;56:96112. Available from: https://doi.org/10.1117/1.OE.56.9.096112.